Adaptive Dynamic Surface Control for Formations of Autonomous Surface Vehicles With Uncertain Dynamics

Zhouhua Peng, Dan Wang, Zhiyong Chen, Xiaojing Hu, and Weiyao Lan

***Abstract*—In this brief, we consider the formation control problem of underactuated autonomous surface vehicles (ASVs) moving in a leader-follower formation, in the presence of uncertainties and ocean disturbances. A robust adaptive formation controller is developed by employing neural network and dynamic surface control technique. The stability of the design is proven via Lyapunov analysis where semiglobal uniform ultimate boundedness of the closed-loop signals is guaranteed. The advantages of the proposed formation controller are that: first, the proposed method only uses the measurements of line-of-sight range and angle by local sensors, no other information about the leader is required for control implementation; second, the developed neural formation controller is able to capture the vehicle dynamics without exact information of coriolis and centripetal force, hydrodynamic damping and disturbances from the environment. Comparative analysis with a model-based approach is given to demonstrate the effectiveness of the proposed method.**

***Index Terms*—Autonomous surface vehicles (ASVs), dynamic surface control, formation control, neural networks (NNs), uncertain dynamics.**

I. Introduction

OVER the past few years, the formation control of multi-vehicle systems attracted great attention in system and control. This is partially due to the fact that there is an increasing need for utilizing multiple vehicles to perform difficult tasks, where it contributes to increasing efficiency, reducing system cost and providing redundancy against individual failure. Relevant applications arising in marine industry include automatic ocean exploration, environmental monitoring, surveillance of territorial waters, underway ship replenishment, and so on. To achieve the desired formation, several methods have been proposed, which include leader-follower strategy [1]–[4], virtual structure method [5], behavioral approach [6], [7], graph theory-based method [8]–[11], artificial potential mechanism [12]–[14], and so on.

Among these control schemes, the leader-follower strategy seems to be much preferred in practice due to its simplicity and scalability [2]. During the last decade, the marine control community has focused on formation control and most of works appear to have been done within the leader-follower framework [15]–[19]. Nonlinear formation control of marine crafts is first considered in [15], where vectorial backstepping is employed to solve the geometric task and dynamics task. Sliding mode control technique is utilized in [16] to develop the leader-follower formation controller for underactuated surface vessels. By applying the integrator backstepping and cascade theory, a guided leader-follower formation control scheme is proposed in [17] for fully actuated vehicles. Using a nonlinear observer to estimate the leader's velocity and acceleration, a leader-follower output synchronization control scheme is developed in [18] for ship replenishment operations. Also, the leader-follower formation control of underactuated autonomous underwater vehicles is reported in [19], where a virtual vehicle is constructed such that its trajectory converges to a reference point. Based on the Lyapunov and backstepping synthesis, an adaptive position tracking law is designed for the follower to track the virtual vehicle.

Although many good results have been obtained, the following are worth mentioning. On one hand, the dynamics of the surface vehicle exhibits some basic properties such as intrinsic nonlinear, strong coupling, multi-input multi-output system, and underactuation. In addition, the marine operations are characterized by time-varying disturbances and widely changing sea condition. Thus, the control design for such nonlinear system is still a challenging problem. Some attempts have been made to solve the above problem based on the traditional adaptive control [21], [22]. However, the uncertainties have to be parametric and time-invariant [23]. Since neural networks (NNs) have an inherent ability of learning nonlinear dynamics [24]–[26], it is attractive to apply them to the control of surface vehicles. The trajectory tracking problem for fully-actuated vessels is considered in [23], where a radial basis function (RBF) NN is employed to handle both the unknown uncertainties and the time-varying disturbances. However, the result based on the fully actuated vehicle is not suitable for underactuated vehicle which is considered in this brief.

On the other hand, the existing leader-follower formation control algorithms rely on the velocity information of the leader [2], [20]. However, in practice, not all the vehicles are equipped with velocity sensors. A formation control algorithm using only position measurements would be much preferred, due to the fact it reduces the equipment cost and also may decrease the network burden [4], [18]. To the implement distance-based

Manuscript received December 21, 2010; revised March 27, 2011; accepted August 31, 2011. Manuscript received in final form December 20, 2011. Date of publication January 31, 2012; date of current version February 14, 2013. Recommended by Associate Editor D. Liu. This work was supported in part by the National Nature Science Foundation of China under Grant 60674037, Grant 61074017, and Grant 61074004 and in part by the Program for Liaoning Excellent Talents in Universities under Grant 2009R06, and by the Fundamental Research Funds for the Central Universities.

Z. Peng and D. Wang are with the School of Marine Engineering, Dalian Maritime University, Dalian 116026, China (e-mail: zhouhuapeng@gmail.com; dwangdl@gmail.com).

Z. Chen is with the School of Electrical Engineering and Computer Science, The University of Newcastle, Callaghan NSW 2308, Australia, and also with the State Key Laboratory of Digital Manufacturing Equipment and Technology, Huazhong University of Science and Technology, China (e-mail: zhiyong.chen@newcastle.edu.au).

X. Hu is with the Liaoning Entry-Exit Inspection and Quarantine Bureau of People's Republic of China, Dalian 116001, China (e-mail: jxhu@263.net).

W. Lan is with the Department of Automation, Xiamen University, Xiamen 361005, China (e-mail: wylan@xmu.edu.cn).

Color versions of one or more of the figures in this brief are available online at http://ieeexplore.ieee.org.

Digital Object Identifier 10.1109/TCST.2011.2181513

formation control algorithm, adaptive control schemes have been suggested [4], [30], [31]. In our previous paper [30], we proposed an adaptive formation control law for multiple autonomous surface vehicles moving in a leader-follower formation. NNs are trained online to compensate for the uncertainties due to the unknown velocities of leader. However, the kinetics of the vehicle dynamics and possible uncertainty in the kinetics are not considered. This work is later extended to formation control of ASVs with uncertain leader dynamics and uncertain local dynamics in [32], where backstepping-based NN control technique is employed to stabilize formations. However, the controller is complicated for the sake of the needs to calculate numerical derivatives of virtual control signals.

In contrast, in this brief we develop an adaptive formation controller for underactuated ASVs, using the NN-based dynamic surface control (DSC) approach [27], [29]. The DSC approach proposed in [27] simplifies the controller design by introducing the first-order filters and avoids the calculation of derivatives of virtual control signals, and is incorporated into NN-based adaptive control framework in [29]. Our NN-based DSC approach applies to the formation control of ASVs, each of which has unknown nonlinear dynamics and subjects to disturbances from the environment. Nonlinearly parameterized NNs are utilized to accommodate the unknown uncertain dynamics. The stability of the system is proven via Lyapunov theory. The main contributions of this brief are as follows.

1) For the first time, the NN-based DSC technique is employed to solve the leader-follower formation control problem of ASVs with uncertain local dynamics and uncertain leader dynamics, which leads to a much simpler formation controller than traditional backstepping-based design.
2) The developed formation controller is universal and model independent, while those developed in [15], [17], and [18] depend on the accurate model of vehicle which is not available in practice.
3) Moreover, the proposed control scheme only depends on the position information of leader, which requires less information than those developed in [2] and [20].

This brief is organized as follows. Section II states the problem formulation. Section III presents the NN formation controller design. Section IV gives the main result. Section V presents the simulation result. Section VI concludes this brief.

II. Problem Formulation and Preliminaries

Notation: Throughout this brief, $\mathbb{R}^n$ denotes the n-dimensional Euclidean space. $\|\cdot\|$ denotes the Euclidean norms. $\|\cdot\|_F$ denotes the Frobenius norm. $(\cdot)_{ij}$ denotes the element of $(\cdot)$ in row i, column j. $\lambda_{\min}(\cdot)$ denotes the smallest eigenvalues of a square matrix $(\cdot)$. Let $X=[x_1,\ldots,x_N]^T$, $Y=[y_1,\ldots,y_N]^T$. Then, we say $X\le Y$ if and only if $x_i\le y_i$, for all i, $1\le i\le N$. $|X|$ denotes $[|x_1|,\ldots,|x_N|]^T$.

A. Vehicle Dynamics

Consider a group of N underactuated ASVs governed by the following dynamics found in [34] with kinematics:

$$\dot{\eta}_i = J(\psi_i)\nu_i \tag{1}$$

and kinetics

$$M_i\dot{\nu}_i + C_i(\nu_i)\nu_i + D_i(\nu_i)\nu_i + g_i(\nu_i) = \tau_i + \tau_{iw} \tag{2}$$

where

$$\begin{aligned}
&\eta_i = [x_i, y_i, \psi_i]^T, \nu_i = [u_i, v_i, r_i]^T,\ \tau_i = [\tau_{iu}, 0, \tau_{ir}]^T\\
&\tau_{iw} = [\tau_{iwu}, \tau_{iwv}, \tau_{iwr}]^T, g_i(\nu_i) = [g_u, g_v, g_r]^T\\
&M_i = \begin{bmatrix} m_{11i} & 0 & 0\\ 0 & m_{22i} & m_{23i}\\ 0 & m_{32i} & m_{33i}\end{bmatrix},\ C_i = \begin{bmatrix} 0 & 0 & c_{13i}\\ 0 & 0 & c_{23i}\\ c_{31i} & c_{32i} & 0\end{bmatrix}\\
&D_i = \begin{bmatrix} d_{11i} & 0 & 0\\ 0 & d_{22i} & d_{23i}\\ 0 & d_{32i} & d_{33i}\end{bmatrix},\ J = \begin{bmatrix} \cos\psi_i & -\sin\psi_i & 0\\ \sin\psi_i & \cos\psi_i & 0\\ 0 & 0 & 1\end{bmatrix}.
\end{aligned}$$

$\eta_i\in\mathbb{R}^3$ is the position vector in the earth-fixed reference frame; $\nu_i\in\mathbb{R}^3$ is the velocity vector in the body-fixed reference frame; $M_i\in\mathbb{R}^{3\times3}$ is the inertia matrix; $C_i(\nu_i)\in\mathbb{R}^{3\times3}$, $D_i(\nu_i)\in\mathbb{R}^{3\times3}$, $g_i(\nu_i)\in\mathbb{R}^3$ denotes the coriolis and centripetal matrix, damping matrix and unmodelled dynamics, respectively, and their entries are functions of ν_i; $\tau_i\in\mathbb{R}^3$ is the control vector with τ_{iu} the surge force and τ_{ir} the yaw moment; $\tau_{iw}\in\mathbb{R}^3$ denotes the disturbances from the environment.

By choosing appropriate body-fixed frame origin as in [22], m_{23i} can be made to satisfy $m_{23i}=0$. As such, the vehicle dynamics in (1) and (2) is represented by

$$\dot{x}_i = u_i\cos\psi_i - v_i\sin\psi_i \tag{3}$$
$$\dot{y}_i = u_i\sin\psi_i + v_i\cos\psi_i \tag{4}$$
$$\dot{\psi}_i = r_i \tag{5}$$
$$\bar{M}_i\dot{\bar{\nu}}_i = -\bar{C}_i\nu_i - \bar{D}_i\nu_i - \bar{g}(\nu_i) + \bar{\tau}_i + \bar{\tau}_{iw} \tag{6}$$
$$m_{22i}\dot{v}_i = -c_{23i}r_i - d_{22i}v_i - d_{23i}r_i - g_v + \tau_{iwv} \tag{7}$$

where $\bar{\nu}_i=[u_i,r_i]^T\in\mathbb{R}^2$, $\bar{\tau}_i=[\tau_{iu},\tau_{ir}]^T\in\mathbb{R}^2$, and the matrix $\bar{M}_i\in\mathbb{R}^{2\times2}$, $\bar{C}_i\in\mathbb{R}^{2\times3}$, $\bar{D}_i\in\mathbb{R}^{2\times3}$, $\bar{\tau}_{iw}\in\mathbb{R}^2$ are continuous with

$$\begin{aligned}
&\bar{M}_i = \begin{bmatrix} m_{11i} & 0\\ 0 & m_{33i}\end{bmatrix} \bar{C}_i = \begin{bmatrix} 0 & 0 & c_{13i}\\ c_{31i} & c_{32i} & -m_{32i}m_{22i}^{-1}c_{23i}\end{bmatrix}\\
&\bar{D}_i = \begin{bmatrix} d_{11i} & 0 & 0\\ 0 & d_{32i}-m_{32i}m_{22i}^{-1}d_{22i} & d_{33i}-m_{32i}m_{22i}^{-1}d_{23i}\end{bmatrix}\\
&\bar{g} = \begin{bmatrix} g_u\\ g_r - m_{32i}m_{22i}^{-1}g_v\end{bmatrix}, \bar{\tau}_{iw} = \begin{bmatrix} \tau_{iwu}\\ \tau_{iwr} - m_{32i}m_{22i}^{-1}\tau_{iwv}\end{bmatrix}.
\end{aligned}$$

B. Leader-Follower Formation

Fig. 1 presents the basic geometric structure about two ASVs moving in a leader-follower formation. The line-of-sight (LOS) range ρ_{ij} and angle λ_{ij} between the leader j and the follower i are defined as

$$\rho_{ij} = \sqrt{(x_j-x_i)^2 + (y_j-y_i)^2} \tag{8}$$
$$\lambda_{ij} = atan2(y_j-y_i, x_j-x_i) \tag{9}$$

where $atan2(y,x)$ returns the arc tangent of y/x with a continuous range of $(-\pi,\pi]$. The formation control presented in this

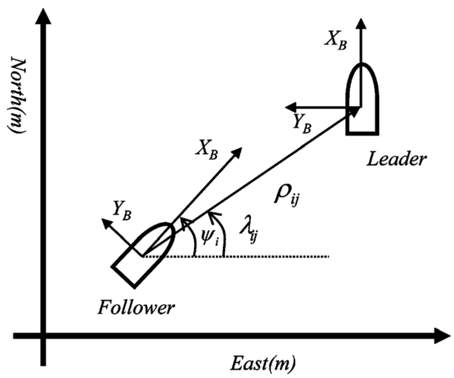

Fig. 1. Leader-follower formation.

brief is based on the measurements of LOS range and angle between the leader and the follower. Thus, define the output vector of formation as

$$s_{ij}(t) = [\rho_{ij}, \lambda_{ij}]^T \tag{10}$$

and the desired output vector of formation as

$$s_{ijd}(t) = [\rho_{ijd}, \lambda_{ijd}]^T \tag{11}$$

where $s_{ij} \in \mathbb{R}^2$, $s_{ijd} \in \mathbb{R}^2$.

Control Objective: The control goal is bounded tracking with the prescribed formation specification. Specifically, the objective is to design a control input τ_i for the follower i to track its leader j with commanded LOS range and angle s_{ijd}, in the presence of uncertain system dynamics and uncertain leader dynamics, and to guarantee that the formation tracking error can be made arbitrarily small.

To move on, we make use of the following assumptions.

Assumption 1: The unknown disturbance $\bar{\tau}_{iw}$ is bounded by $|\bar{\tau}_{iw}| \le \bar{\tau}_{iM}$, where $\bar{\tau}_{iM} \in \mathbb{R}^2$ is a positive constant vector.

Definition 1 [21]: Consider a system $\dot{x}_i = f(X) + d$, where $X = [x_1, \ldots, x_i, \ldots, x_n]^T$, $f : \mathbb{R}^n \to \mathbb{R}$ is a function and d is a disturbance term. For all bounded x_j, $j \ne i$ and d, if there exists a scalar function $V(x_i) \in C^1$ such that it follows:

1) $V(x_i)$ is globally positive definite and further radially unbounded;
2) $\dot{V}(x_i) < 0$ if $|x_i| > b$, where b is a positive constant and its magnitude is related to the bounds of x_j, $j \ne i$ and d;

then the variable x_i is passive-bounded.

Assumption 2: The sway velocity of vehicle is passive-bounded.

Assumption 3: The formation specification is bounded and satisfies $[s_{ijd}^T, \dot{s}_{ijd}^T, \ddot{s}_{ijd}^T]^T \in \Omega_d$ with $\Omega_d = \{[s_{ijd}^T, \dot{s}_{ijd}^T, \ddot{s}_{ijd}^T]^T$: $\|s_{ijd}\|^2 + \|\dot{s}_{ijd}\|^2 + \|\ddot{s}_{ijd}\|^2 \le B_0\} \subset \mathbb{R}^6$, where B_0 is a positive constant.

Remark 1: Although the bounds mentioned above are assumed to exist, their values are not used in the controller and do not have to be known. Passive-boundedness of the sway dynamics has been systematically analyzed considering different cases in [21]. This assumption is highly realistic since in practice the hydrodynamic damping force dominates in the sway direction and the sway speed is damped out by this force. Following [21], we make the same assumption on the sway dynamics.

III. NN Formation Controller Design

In this section, we present the leader-follower formation control algorithm based on NN-based DSC technique [27], [29]. Similar to the traditional backstepping design approach, the controller design contains three steps. The overall control law is constructed at step 3. Before designing the controller, we shall derive the relative dynamics between the leader and follower from the kinematics (1). By differentiating (10) and using (1), the relative dynamics can be described by

$$\dot{s}_{ij} = B(\omega_i + \Delta_i),\ s_{ij}(0) = s_0 \tag{12}$$

where $B \in \mathbb{R}^{2\times 2}$, $\omega_i = [\omega_{i1}, \omega_{i2}]^T \in \mathbb{R}^2$, $\Delta_i \in \mathbb{R}^2$ are given by

$$B = \begin{bmatrix} -1 & 0 \\ 0 & \frac{-1}{\rho_{ij}} \end{bmatrix}, \omega_i = \begin{bmatrix} u_i \cos(\psi_i - \lambda_{ij}) \\ u_i \sin(\psi_i - \lambda_{ij}) \end{bmatrix} \tag{13}$$

$$\begin{aligned} \Delta_i &= \begin{bmatrix} -u_j \cos(\psi_j - \lambda_{ij}) + v_j \sin(\psi_j - \lambda_{ij}) \\ -u_j \sin(\psi_j - \lambda_{ij}) - v_j \cos(\psi_j - \lambda_{ij}) \end{bmatrix} \\ &\quad + \begin{bmatrix} -v_i \sin(\psi_i - \lambda_{ij}) \\ v_i \cos(\psi_i - \lambda_{ij}) \end{bmatrix} \\ &\le \begin{bmatrix} |u_j| + |v_j| + |v_i| \\ |u_j| + |v_j| + |v_i| \end{bmatrix}. \end{aligned} \tag{14}$$

Here, the leader states u_j, v_j are not available for the follower i, and they can be treated as external disturbances imposed on subsystem (12). As the leader moves in the sea and subjects to the hydrodynamic damping force, the surge speed of leader u_j cannot be infinite and is bounded. Together with Assumption 2, it follows from (14) that there exists a positive constant vector $\varrho_i \in \mathbb{R}^2$ such that $|\Delta_i| \le \varrho_i$.

Step 1: At this step, the goal is to make s_{ij} track the desired formation s_{ijd}. To this end, let $s_{ije} = s_{ij} - s_{ijd} \in \mathbb{R}^2$, whose time derivative satisfies

$$\dot{s}_{ije} = -\dot{s}_{ijd} + B(\omega_i + \Delta_i). \tag{15}$$

To facilitate the stability analysis, consider a scalar function $V_1 = (1/2)s_{ije}^T s_{ije}$, whose time derivative along (15) is given by

$$\begin{aligned} \dot{V}_1 &= s_{ije}^T[-\dot{s}_{ijd} + B(\omega_i + \Delta_i)] \\ &\le s_{ije}^T(-\dot{s}_{ijd} + B\omega_i) + |s_{ije}^T B|\varrho_i. \end{aligned} \tag{16}$$

Using the inequality $|x| - x\tanh(x/\backepsilon) \le 0.2785\ \backepsilon$ with $\backepsilon$ a positive constant, we have

$$|s_{ije}^T B| - s_{ije}^T B Y_1(s_{ije}, s_{ij}) \le 0.2785\delta^T \tag{17}$$

where $Y_1(s_{ije}, s_{ij}) = \mathrm{diag}\{\tanh(s_{ije}^T B)_{11}/\delta_1, \tanh(s_{ije}^T B)_{12}/\delta_2\}$, $\delta = [\delta_1, \delta_2]^T$, and δ_1, δ_2 are positive constants. Then, (16) becomes

$$\dot{V}_1 \le s_{ije}^T(-\dot{s}_{ijd} + B\omega_i) + s_{ije}^T B Y_1(\cdot)\varrho_i + 0.2785\delta^T\varrho_i. \tag{18}$$

Choose the *kinematic control law* as

$$\bar{\omega}_i = B^{-1}(\dot{s}_{ijd} - k_s s_{ije}) - Y_1(\cdot)\hat{\varrho}_i \tag{19}$$

and the adaptive law

$$\dot{\hat{\varrho}}_i = \Gamma_{\varrho_i}[Y_1(\cdot)B^T s_{ije} - k_{\varrho_i}\hat{\varrho}_i] \tag{20}$$

where $k_s > 0, \Gamma_{\varrho_i} > 0, k_{\varrho_i} > 0$, and $\hat{\varrho}_i$ is the estimate of ϱ_i. Let $\bar{\omega}_i = [\bar{u}_i\cos(\bar{\psi}_i - \lambda_{ij}), \bar{u}_i\sin(\bar{\psi}_i - \lambda_{ij})]^T$, where $\bar{u}_i$ and $\bar{\psi}_i$ are virtual control signals and they can be solved as

$$\bar{\psi}_i = \lambda_{ij} + atan2(\bar{\omega}_{i2}, \bar{\omega}_{i1}) \tag{21}$$
$$\bar{u}_i = \cos(\bar{\psi}_i - \lambda_{ij})\bar{\omega}_{i1} + \sin(\bar{\psi}_i - \lambda_{ij})\bar{\omega}_{i2}. \tag{22}$$

Introduce two new state variables ψ_{id}, u_{id} and let $\bar{\psi}_i$, $\bar{u}_i$ pass through two first-order filters with time constants γ_1, γ_2 to obtain ψ_{id}, u_{id}, respectively

$$\gamma_1\dot{\psi}_{id} = \bar{\psi}_i - \psi_{id}, \gamma_2\dot{u}_{id} = \bar{u}_i - u_{id} \tag{23}$$

where $\gamma_1 > 0, \gamma_2 > 0$. Let

$$\psi_{ie} = \psi_i - \psi_{id}, u_{ie} = u_i - u_{id} \tag{24}$$
$$z_1 = \psi_{id} - \bar{\psi}_i, z_2 = u_{id} - \bar{u}_i. \tag{25}$$

Then, consider the second scalar function

$$V_2 = V_1 + \frac{1}{2}\tilde{\varrho}_i^T\Gamma_{\varrho_i}^{-1}\tilde{\varrho}_i + \frac{1}{2}z_1^2 + \frac{1}{2}z_2^2 \tag{26}$$

whose time derivative along (19) and (20) is given by

$$\begin{aligned}\dot{V}_2 \le& -\lambda_{\min}(k_s)\|s_{ije}\|^2 + 0.2785\delta^T\varrho_i + z_2\dot{z}_2\\ &+ z_1\dot{z}_1 + \|s_{ije}\|\|B(\omega_i - \bar{\omega}_i)\| - k_{\varrho_i}\tilde{\varrho}_i^T\hat{\varrho}_i.\end{aligned} \tag{27}$$

Step 2: This step aims to stabilize the yaw tracking error ψ_{ie}. By differentiating the first equation in (24) along (5), we obtain

$$\dot{\psi}_{ie} = r_i - \dot{\psi}_{id}. \tag{28}$$

Choose the following yaw rate control law:

$$\bar{r}_i = \dot{\psi}_{id} - k_r\psi_{ie} \tag{29}$$

where $k_r > 0$. Introduce a new state r_{id} and let $\bar{r}_i$ pass through a first order filter with a time constant γ_3 to obtain r_{id}

$$\gamma_3\dot{r}_{id} = \bar{r}_i - r_{id} \tag{30}$$

where $\gamma_3 > 0$. Let

$$r_{ie} = r_i - r_{id}, z_3 = r_{id} - \bar{r}_i \tag{31}$$

where r_{ie} represents the tracking error of yaw rate. Now, consider the third scalar function as

$$V_3 = V_2 + \frac{1}{2}\psi_{ie}^2 + \frac{1}{2}z_3^2 \tag{32}$$

whose time derivative along (29) and (31) is

$$\dot{V}_3 = \dot{V}_2 + \psi_{ie}(r_{ie} + z_3) - k_r\psi_{ie}^2 + z_3\dot{z}_3. \tag{33}$$

Step 3: The final control law will be derived at this step. First, let $\bar{\nu}_{ie} = [u_{ie}, r_{ie}]^T$ and it follows from (6), (31), and (24) that the time derivative of $\bar{\nu}_{ie}$ is

$$\bar{M}_i\dot{\bar{\nu}}_{ie} = -\bar{C}_i\nu_i - \bar{D}_i\nu_i - \bar{g}(\nu_i) - \bar{M}_i[\dot{u}_{id}, \dot{r}_{id}]^T + \bar{\tau}_i + \bar{\tau}_{iw}. \tag{34}$$

Consider the fourth scalar function

$$V_4 = V_3 + \frac{1}{2}\bar{\nu}_{ie}^T\bar{M}_i\bar{\nu}_{ie} \tag{35}$$

whose time derivative along (34) is given by

$$\begin{aligned}\dot{V}_4 \le& \dot{V}_3 + \bar{\nu}_{ie}^T\{-\bar{C}_i\nu_i - \bar{D}_i\nu_i - \bar{g}(\nu_i)\\ &- \bar{M}_i[\dot{u}_{id}, \dot{r}_{id}]^T + \bar{\tau}_i\} + |\bar{\nu}_{ie}^T|\bar{\tau}_{iM}.\end{aligned} \tag{36}$$

Similarly, using the property of $\tanh(\cdot)$, we have

$$|\bar{\nu}_{ie}^T| - \bar{\nu}_{ie}^T Y_2(\bar{\nu}_{ie}) \le 0.2785\delta^T \tag{37}$$

where $Y_2(\bar{\nu}_{ie})$=diag$\{\tanh(\bar{\nu}_{ie}^T)_{11}/\delta_1, \tanh(\bar{\nu}_{ie}^T)_{12}/\delta_2\}$. Then, (36) becomes

$$\dot{V}_4 \le \dot{V}_3 + \bar{\nu}_{ie}^T\{f_i(\xi_i) + \bar{\tau}_i\} + 0.2785\delta^T\bar{\tau}_{iM} \tag{38}$$

where $f_i(\xi_i) = -\bar{M}_i[\dot{u}_{id}, \dot{r}_{id}]^T - \bar{C}_i\nu_i - \bar{D}_i\nu_i - \bar{g}(\nu_i) + Y_2(\cdot)\bar{\tau}_{iM}$ with $\xi_i = [\nu_i^T, \bar{\nu}_{ie}^T, \dot{u}_{id}, \dot{r}_{id}, 1]^T \in \mathbb{R}^8$. On the condition that $\bar{g}(\nu_i)$ and $\bar{\tau}_{iM}$ are unknown, $f_i(\nu_i)$ is not available; in what follows, $f_i(\xi_i)$ can be approximated by a single hidden layer (SHL) NN [25], [28] as

$$f_i(\xi_i) = W_i^T\sigma(V_i^T\xi_i) + \epsilon_i(\xi_i) \tag{39}$$

where $\epsilon_i(\xi_i)$ is the approximation error satisfying $\|\epsilon_i(\xi_i)\| \le \epsilon_{iM}$ with ϵ_{iM} a positive constant. Rewrite (38) as

$$\dot{V}_4 \le \dot{V}_3 + \bar{\nu}_{ie}^T\{W_i^T\sigma(V_i^T\xi_i) + \epsilon_i + \bar{\tau}_i\} + 0.2785\delta^T\bar{\tau}_{iM}. \tag{40}$$

Select the following *kinetic control law*

$$\bar{\tau}_i = -\hat{W}_i^T\sigma\left(\hat{V}_i^T\xi_i\right) - k_\nu\bar{\nu}_{ie} - h_i \tag{41}$$

with adaptive laws

$$\begin{aligned}\dot{\hat{W}}_i =& \Gamma_{W_i}\left[\left(\hat{\sigma} - \hat{\sigma}'\hat{V}_i^T\xi_i\right)\bar{\nu}_{ie}^T - k_{W_i}\hat{W}_i\right]\\ \dot{\hat{V}}_i =& \Gamma_{V_i}\left[\xi_i\bar{\nu}_{ie}^T\hat{W}_i^T\hat{\sigma}' - k_{V_i}\hat{V}_i\right]\end{aligned} \tag{42}$$

where $k_\nu > 0, k_{W_i} > 0, k_{V_i} > 0, \Gamma_{W_i} > 0, \Gamma_{V_i} > 0$ and h_i is an auxiliary function defined as $h_i = k_{i1}(\|\xi_i\hat{W}_i^T\hat{\sigma}'\|_F^2 + \|\hat{\sigma}'\hat{V}_i^T\xi_i\|^2 + 1)\bar{\nu}_{ie}$. $\hat{W}_i, \hat{V}_i$ are the estimates of unknown parameters W_i, V_i, respectively. Letting $\tilde{W}_i = W_i - \hat{W}_i, \tilde{V}_i = V_i - \hat{V}_i$ and taking the similar approach as in [28], we have

$$\begin{aligned}W_i^T\sigma\left(V_i^T\xi_i\right) - \hat{W}_i^T\sigma\left(\hat{V}_i^T\xi_i\right) =& \tilde{W}_i^T\left(\hat{\sigma} - \hat{\sigma}'\hat{V}_i^T\xi_i\right)\\ &+ \hat{W}_i^T\hat{\sigma}'\tilde{V}_i^T\xi_i + d_i\end{aligned} \tag{43}$$

where $\|d_i\| \leq a_1\|\xi_i \hat{W}_i^T \hat{\sigma}'\|_F + a_2\|\hat{\sigma}'\hat{V}_i^T\xi_i\| + a_3$ with a_1, a_2, a_3 constants. Then, (40) with (41) and (43) is

$$\dot{V}_4 \leq \dot{V}_3 - k_\nu\|\bar{\nu}_{ie}\|^2 + \bar{\nu}_{ie}^T\{\tilde{W}_i^T\left(\hat{\sigma} - \hat{\sigma}'\hat{V}_i^T\xi_i\right) + \hat{W}_i^T\hat{\sigma}'\tilde{V}_i^T\xi_i + \epsilon_i + d_i - h_i\} + 0.2785\delta^T\bar{\tau}_{iM}. \quad (44)$$

Remark 2: By incorporating the DSC technique, our design leads to a much simpler formation controller than the traditional backstepping-based design. In fact, using the traditional backstepping-based method, the higher order derivatives of $\bar{\psi}_i$, $\bar{u}_i$, $\bar{r}_i$ would have to appear in the kinetic controller $\bar{\tau}_i$. As a result, the expression of the $\bar{\tau}_i$ would be much more complicated. The "explosion of complexity" problem is serious in this case though the system order is two due to the multi-input multi-output characteristics of the system.

Remark 3: The paper [21] considered the robust point-to-point navigation of marine ships. The vehicle kinetics in [21] only contains the linearly parameterized uncertainty, i.e, the uncertain parts of the kinetics are in form of $\theta^T f(\cdot)$, where θ is an unknown constant and $f(\cdot)$ is a known smooth function. Therefore, the adaptive control given in [21] cannot apply to our case where the uncertain part $\bar{g}(\nu_i)$ is totally unknown.

IV. Main Result

In this section, we have the main result stated as follows.

Theorem 1: Consider the closed-loop system consisting of the vehicle dynamics in (1) and (2) under Assumptions 1–3, and the control laws in (19), (29), (41), adaptive laws in (20) and (42) and low pass filters in (23) and (30). Given any positive number p, for bounded initial conditions satisfying $V(0) \leq p$, there exist $k_s > 0$, $k_r > 0$, $k_\nu > 0$, $\Gamma_{\varrho_i} > 0$, $\Gamma_{W_i} > 0$, $\Gamma_{V_i} > 0$, $k_{\varrho_i} > 0$, $k_{W_i} > 0$, $k_{V_i} > 0$, such that the solution of the closed-loop system is uniformly ultimately bounded, and the steady-state formation tracking error can be made arbitrarily small.

Proof: By constructing the following Lyapunov function candidate

$$V = V_4 + \frac{1}{2}tr\left\{\tilde{W}_i^T\Gamma_{W_i}^{-1}\tilde{W}_i\right\} + \frac{1}{2}tr\left\{\tilde{V}_i^T\Gamma_{V_i}^{-1}\tilde{V}_i\right\} \quad (45)$$

the uniform ultimate boundedness of the closed-loop system can be established. The proof is similar to [29] and is omitted here to save space.

Remark 4: To improve the formation tracking performance, the following design guidelines are provided.

1) Appropriately increasing the number of NN nodes will decrease the function approximation error, which will consequently result in a smaller tracking error.
2) The control parameters for $k_s, k_\nu, k_r, \Gamma_{W_i}, \Gamma_{V_i}, \Gamma_{\rho_i}$ can be increased such that the tracking errors in the steady phase also can be reduced.

V. Simulation Results

In this section, an example is given to illustrate the method. The dynamical model of an experimental surface vehicle used in [22] is considered. In addition, some model uncertainties and time-varying disturbances are introduced into the model, in particular, $g_i = [0.0122uv + 0.0142v^2, 0.09v^2r, 0.0257ur + 0.0193r^2v]^T$ and $\tau_{iw} = [-3\cos(0.5t)\cos(t) + 0.3\sin(0.3t)\cos(0.8t) -3, 0.1\cos(0.1t), 0.6\sin(t)\cos(0.2t)]^T$. We consider five vehicles governed by the above model to shape a formation. In the formation setup, one vehicle is designated as leader ($j = 5$), another four vehicles as followers ($i = 1,2,3,4$). Similar to [26], a first order command filter is implemented to obtain s_{ijd}, $\dot{s}_{ijd}$ so that $s_{ijd} = [c/s + c]s_{ijc}$ with $c = 0.1$. The commanded formation is $s_{15c} = [2, -45°]^T$, $s_{25c} = [2, 45°]^T$, $s_{35c} = [4, -45°]^T$, $s_{45c} = [4, 45°]^T$. The initial positions corresponding to the five vehicles are $F_1 = [0, 4]$, $F_2 = [0, -4]$, $F_3 = [0, 6]$, $F_4 = [0, -6]$, $L_5 = [4, 0]$.

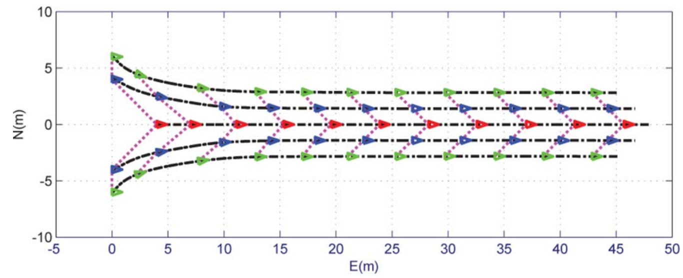

Fig. 2. Formation trajectories in 2-D plane. L5(red), F1 and F2 (blue), F3 and F4 (green).

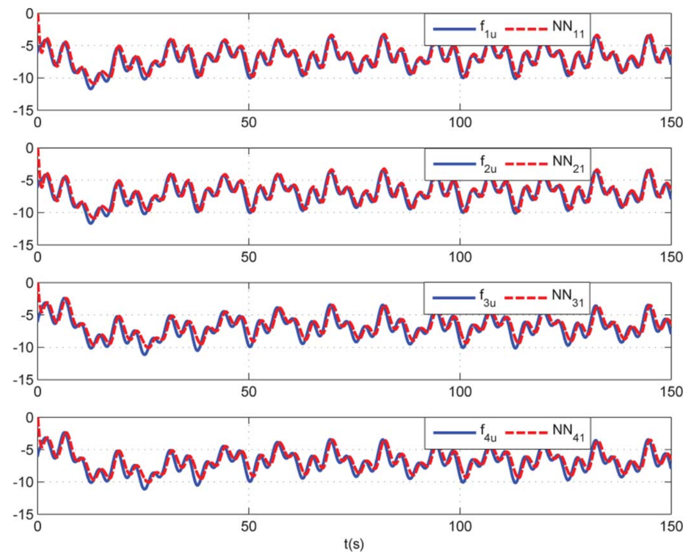

Fig. 3. NN approximate the uncertain dynamics in the surge direction.

Below, we discuss how to choose the number of neurons and control parameters. In general, as in most control system, the performance can be improved by trying a few simulation runs and adjusting the parameters to obtain good behavior. The number of neurons is selected as follows. The simulation was first performed with eight neurons. Then, six neurons were used and it was found that the approximation performance degraded. On the other hand, a simulation using 12 neurons did not improve the approximation performance dramatically. Therefore, eight neurons were selected. For the NN activation function, we use the sigmoid basic function of the form $1/[1 + \exp(-x)]$. At the beginning, the NN weights were initialized with zero. Once started, the NN weights can be adjusted online to obtain better

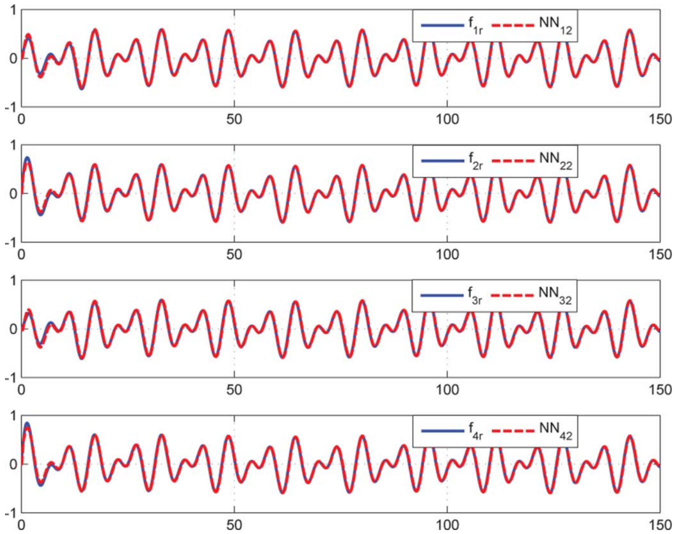

Fig. 4. NN approximate the uncertain dynamics in the yaw direction.

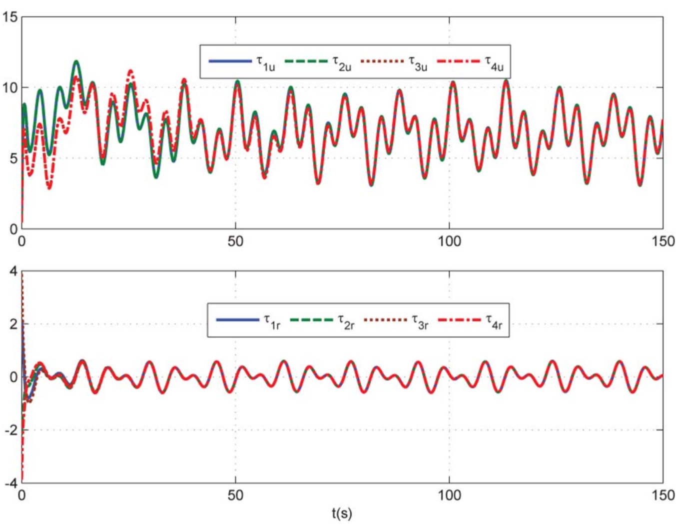

Fig. 5. Control efforts with respect to the four followers.

performance. For control parameters, by Remark 4, we know the control gains should be selected large and another consideration is that the adaptive terms should be faster than the proportional terms such that a good approximation can be obtained. Therefore, the adaptive gains are taken as $\Gamma_{\varrho_i} = 100$, $\Gamma_{W_i} = 100$, $\Gamma_{V_i} = 100$, $\Gamma_{\varrho_i} = 100$, $k_{\varrho_i} = 0.5$, $k_{W_i} = 0.1$, $k_{V_i} = 0.1$, $k_{\varrho_i} = 0.5$. Accordingly, the proportional gains are taken as $k_s = \mathrm{diag}\{5, 5\}$, $k_r = 2$, $k_\nu = \mathrm{diag}\{51.6, 13.8\}$. In theory, increasing adaptive gains will result in a better tracking performance, however, our numerical experience indicates that very large adaptive gains would lead to unexpected large control signals in the initial stage. The parameters for the first order filters are selected as $\gamma_1 = 0.1$, $\gamma_2 = 0.1$, $\gamma_3 = 0.05$.

A. Closed-Loop Performance

Simulation results are shown in Figs. 2–7 and 9. Fig. 2 demonstrates the entire formation trajectories where the leader is commanded in a straight line with constant velocity $u_5 = 0.3$ m/s. It indicates that the formation is well established despite

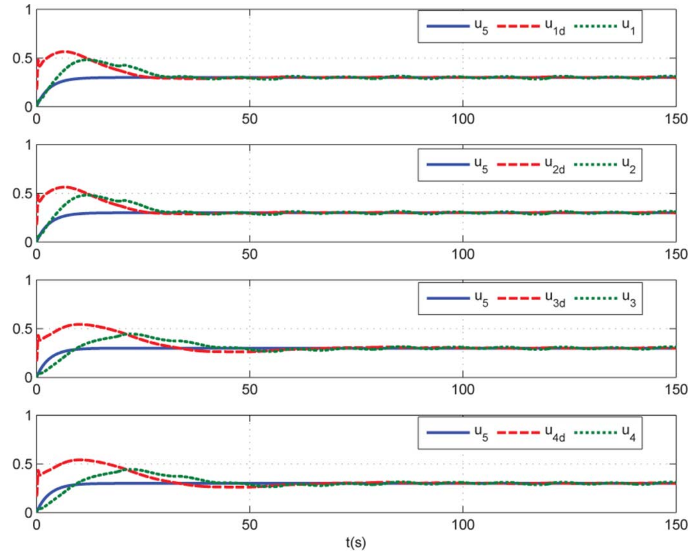

Fig. 6. Surge velocities of followers versus leader.

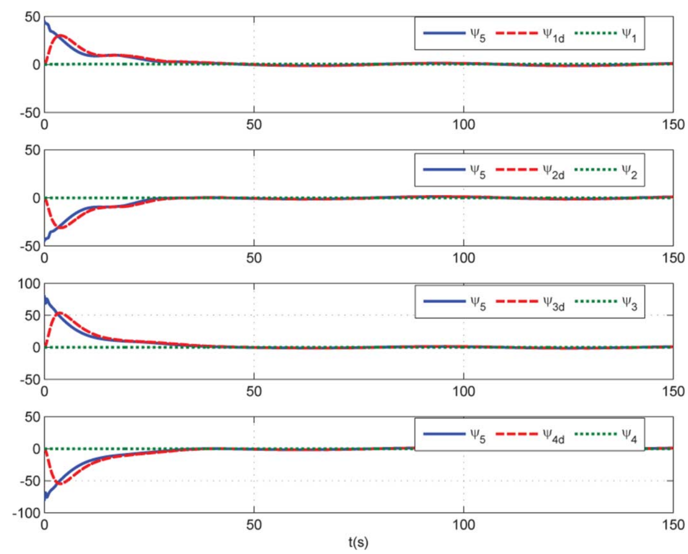

Fig. 7. Yaw angles of followers versus leader.

the existence of the time-varying disturbances and unmodelled dynamics. Figs. 3 and 4 show the learning behavior of NNs. It can be observed that the local uncertainties in the surge and yaw direction are efficiently compensated by the outputs of NNs. Fig. 5 shows that the control efforts with surge force are bounded within 0–15 N, and the yaw moments are bounded within ± 4 Nm. In [23], both the surge and sway control signals are saturated due to the initial tracking error as well as the effects of the high-gain observer and approximation. To handle this, some limiters are introduced to prevent the control saturation. However, introducing limiters may deteriorate the desired performance. A recently developed technique of pseudo-control hedging allows prevention of the saturation through modification of the reference model [33]. We incorporate this technique in simulation. Consequently, Fig. 5 confirms that the level of control activity is reasonable, and no saturation has occurred during the adaptation process. Figs. 6 and 7 show that after several seconds, the followers are able to capture the motion of

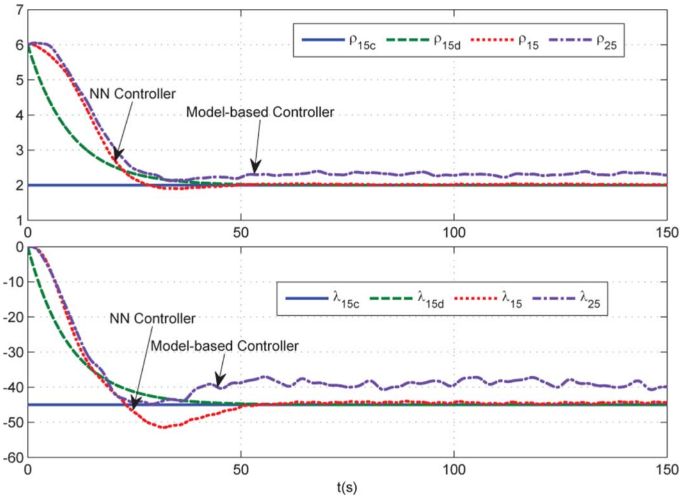

Fig. 8. Comparison with model-based control.

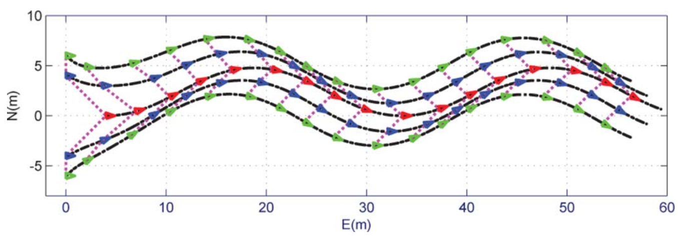

Fig. 9. Formation trajectories in 2-D plane when the leader is commanded in a sinusoid.

the leader. Fig. 9 describes the formation trajectories in the case that the motion of the leader is commanded in a sinusoid, and one can easily see that the formation is also well established.

B. Comparison With Model-Based Controller

In this subsection, the proposed NN-based controller is compared with the model-based controller. Many good results for formation control of marine surface vehicles rely on model-based approaches [15], [17]. The model-based kinetic controller with exact knowledge of $\bar{M}_i$, $\bar{C}_i$, $\bar{D}_i$ is given by

$$\bar{\tau}_{imb} = \bar{M}_i[\dot{u}_{id}, \dot{r}_{id}]^T + \bar{C}_i\nu_i + \bar{D}_i\nu_i - k_\nu\bar{\nu}_{ie}. \quad (54)$$

For comparison, the NN controller (19), (29), (41) is applied to vehicle 1 and the model-based controller (19), (29), (54) is applied to vehicle 2. The initial position of the two vehicles are $F_1 = F_2 = [0, 0]$ and the commanded formation $s_{15c} = s_{25c} = [2, -45°]^T$. Fig. 8 shows the simulation results between the two controllers. It can be observed that the NN-based controller performs better than the model-based controller, with a smaller steady tracking error. The better performance is accounted for that the external disturbance and unmodelled dynamics are efficiently compensated by NNs. In contrast, $\bar{\tau}_{imb}$ does not have an adaptive term to compensate for them, which consequently results in a larger steady tracking error.

VI. Conclusion

This brief presents an NN-based DSC approach for formation control of underactuated autonomous surface vehicles, in the presence of the uncertain local dynamics as well as uncertain leader dynamics. Compared with the existing results, the NN-based DSC scheme shows some advantages to handle these uncertainties and avoid the computation of virtual control derivatives. Based on Lyapunov stability theory, the developed formation controller guarantees that all signals in the closed-loop system are bounded. Simulation results demonstrate the effectiveness of the formation controller and the learning ability of NN.

Acknowledgment

The authors would like to thank the anonymous reviewers for their constructive comments and suggestions that have improved the quality of this brief.

References

[1] A. Das, R. Fierro, V. Kumar, J. Ostrowski, J. Spletzer, and C. Taylor, "A vision-based formation control framework," *IEEE Trans. Robot. Autom.*, vol. 18, no. 5, pp. 813–825, Oct. 2002.
[2] C. Luca, M. Fabio, P. Domenico, and T. Mario, "Leader-follower formation control of nonholonomic mobile robots with input constraints," *Automatica*, vol. 44, no. 5, pp. 1343–1349, May 2008.
[3] B. Yun, B. M. Chen, K. Y. Lum, and T. H. Lee, "Design and implementation of a leader-follower cooperative control unmanned helicopters," *J. Control Theory Appl.*, vol. 8, no. 1, pp. 61–68, Jan. 2010.
[4] K. Choi, S. J. Yoo, J. B. Park, and Y. H. Choi, "Adaptive formation control in absence of leader's velocity information," *IET Control Theory Appl.*, vol. 4, no. 4, pp. 521–528, Apr. 2010.
[5] R. Beard, J. Lawton, and F. Hadaegh, "A coordination architecture for spacecraft formation control," *IEEE Trans. Control Syst. Technol.*, vol. 9, no. 6, pp. 777–790, Nov. 2001.
[6] T. Balch and R. C. Arkin, "Behavior-based formation control for multirobot teams," *IEEE Trans. Robot. Autom.*, vol. 14, no. 6, pp. 926–939, Dec. 1999.
[7] F. Arrichiello, S. Chiaverini, and T. I. Fossen, "Formation control of underactuated surface vessels using the null-space-based behavioral control," in *Proc. Int. Conf. Intell. Robots Syst.*, Oct. 2006, pp. 5942–5947.
[8] I. F. Ihle, M. Arcak, and T. I. Fossen, "Passivity-based designs for synchronized path following," *Automatica*, vol. 43, no. 9, pp. 1508–1518, Dec. 2007.
[9] J. A. Fax and R. M. Murray, "Information flow and cooperative control of vehicle formations," *IEEE Trans. Autom. Control*, vol. 49, no. 9, pp. 1465–1476, Sep. 2004.
[10] G. Lafferriere, A. Williams, J. Caughman, and J. J. P. Veerman, "Decentralized control of vehicle formations," *Syst. Control Lett.*, vol. 54, no. 9, pp. 899–910, Sep. 2005.
[11] W. Ren, "Consensus strategies for cooperative control of vehicle formations," *IET Control Theory Appl.*, vol. 1, no. 2, pp. 505–512, Mar. 2007.
[12] N. E. Leonard and E. Fiorelli, "Virtual leader, artificial potentials and coordinated control of groups," in *Proc. IEEE Conf. Decision Control*, 2001, pp. 2968–2973.
[13] V. Gazi and R. Ordóñez, "Target tracking using artificial potentials and sliding mode control," *Int. J. Control*, vol. 80, no. 10, pp. 1626–1635, Oct. 2007.
[14] K. D. Do, "Output-feedback formation tracking control of unicycle-type mobile robots with limited sensing ranges," *Robot. Autonomous Syst.*, vol. 57, no. 1, pp. 34–47, Jan. 2009.
[15] R. Skjetne, S. Moi, and T. I. Fossen, "Nonlinear formation control of marine vessel," in *Proc. Conf. Decision Control*, 2002, pp. 1699–1704.
[16] F. Fahimi, "Sliding mode formation control for under-actuated autonomous surface vehicle," in *Proc. Amer. Control Conf.*, 2006, pp. 4255–4260.
[17] M. Breivik, V. E. Hovstein, and T. I. Fossen, "Ship formation control: A guided leader-follower approach," *IFAC World Congr.*, vol. 17, no. 1, pp. 16008–16014, Jul. 2008.
[18] E. Kyrkjebø, K. Y. Pettersen, M. Wondergem, and H. Nijmeijer, "Output synchronization control of ship replenishment operations: Theory and experiments," *Control Eng. Pract.*, vol. 15, no. 6, pp. 741–755, Jun. 2006.

[19] R. Cui, S. S. Ge, B. V. E. How, and Y. S. Choo, "Leader-follower formation control of underactuated autonomous underwater vehicles," *Ocean Eng.*, vol. 37, no. 17–18, pp. 1491–1502, Dec. 2010.

[20] T. Dierks and S. Jagannathan, "Neural network control of mobile robot formations using RISE feedback," *IEEE Trans. Syst., Man, Cybern. B, Cybern.*, vol. 39, no. 2, pp. 332–347, Apr. 2009.

[21] J. H. Li, P. M. Lee, B. H. Jun, and Y. K. Lim, "Point-to-point navigation of underactuated ships," *Automatica*, vol. 44, no. 12, pp. 3201–3205, Dec. 2008.

[22] K. D. Do and J. Pan, "Global robust adaptive path following of underactuated ships," *Automatica*, vol. 42, no. 10, pp. 1713–1722, Oct. 2006.

[23] K. P. Tee and S. Z. Ge, "Control of fully actuated ocean surface vessels using a class of feedforward approximators," *IEEE Trans. Control Syst. Technol.*, vol. 14, no. 4, pp. 750–756, Jul. 2006.

[24] K. Hornik, "Approximation capabilities of multilayer feedforward networks," *Neural Netw.*, vol. 4, no. 2, pp. 251–257, 1991.

[25] F. L. Lewis, A. Yesildirek, and K. Liu, "Multilayer neural-net robot controller with guaranteed tracking performance," *IEEE Trans. Neural Netw.*, vol. 7, pp. 388–399, Mar. 1996.

[26] N. Hovakimyan, F. Nardi, A. Calise, and N. Kim, "Adaptive output feedback control of uncertain systems using hidden layer neural networks," *IEEE Trans. Neural Netw.*, vol. 13, no. 6, pp. 1420–1431, Nov. 2002.

[27] D. Swaroop, J. K. Hedrick, P. P. Yip, and J. C. Gerdes, "Dynamic surface control for a class of nonlinear system," *IEEE Trans. Autom. Control*, vol. 45, no. 10, pp. 1893–1899, Oct. 2000.

[28] D. Wang and J. Huang, "Adaptive neural network control for a class of uncertain nonlinear systems in pure-feedback form," *Automatica*, vol. 38, no. 8, pp. 1365–1372, Aug. 2002.

[29] D. Wang and J. Huang, "Neural network-based adaptive dynamic surface control for a class of uncertain nonlinear systems in strict-feedback form," *IEEE Trans. Neural Netw.*, vol. 6, no. 1, pp. 195–202, Jan. 2005.

[30] Z. H. Peng, D. Wang, Y. B. Yao, W. Y. Lan, X. Q. Li, and G. Sun, "Robust adaptive formation control with autonomous surface vehicles," in *Proc. Chinese Control Conf.*, 2010, pp. 2115–2120.

[31] Z. H. Peng, D. Wang, W. Y. Lan, X. Q. Li, and G. Sun, "Filtering robust adaptive formation guidance of unmanned surface vehicles with uncertain leader dynamics," in *Proc. Int. Conf. Intell. Control Inform. Process.*, 2010, pp. 143–148.

[32] Z. H. Peng and D. Wang, "Robust adaptive formation control of autonomous surface vehicles with uncertain dynamics," *IET Control Theory Appl.*, vol. 5, no. 12, pp. 1378–1387, Aug. 2011.

[33] R. Sattiger and A. J. Calise, "An adaptive vision-based approach to decentralized formation control," in *Proc. AIAA Guid., Nav., Control Conf. Exhibit*, 2004, pp. 2004–5252.

[34] T. I. Fossen, *Marine Control System: Guidance, Navigation and Control of Ships, Rigs and Underwater Vehicles*. Trondheim, Norway: Marine Cyernetics, 2002.